APPLIED AND ENVIRONMENTAL MICROBIOLOGY, Feb. 2001, p. 961–968 Vol. 67, No. 2
0099-2240/01/$04.00+0 DOI: 10.1128/AEM.67.2.961–968.2001

In Situ Accessibility of *Escherichia coli* 23S rRNA to Fluorescently Labeled Oligonucleotide Probes

BERNHARD M. FUCHS,[1]* KAZUAKI SYUTSUBO,[1,2] WOLFGANG LUDWIG,[3] AND RUDOLF AMANN[1]

Max Planck Institute for Marine Microbiology, D-28359 Bremen,[1] and Technical University Munich, Department of Microbiology, D-85350 Freising,[3] Germany, and Marine Biotechnology Institute, Kamaishi Laboratories, Heita, Kamaishi City, Iwate 026-0001, Japan[2]

Received 1 September 2000/Accepted 14 November 2000

One of the main causes of failure of fluorescence in situ hybridization with rRNA-targeted oligonucleotides, besides low cellular ribosome content and impermeability of cell walls, is the inaccessibility of probe target sites due to higher-order structure of the ribosome. Analogous to a study on the 16S rRNA (B. M. Fuchs, G. Wallner, W. Beisker, I. Schwippl, W. Ludwig, and R. Amann, Appl. Environ. Microbiol. 64:4973–4982, 1998), the accessibility of the 23S rRNA of *Escherichia coli* DSM 30083^T was studied in detail with a set of 184 CY3-labeled oligonucleotide probes. The probe-conferred fluorescence was quantified flow cytometrically. The brightest signal resulted from probe 23S-2018, complementary to positions 2018 to 2035. The distribution of probe-conferred cell fluorescence in six arbitrarily set brightness classes (classes I to VI, 100 to 81%, 80 to 61%, 60 to 41%, 40 to 21%, 20 to 6%, and 5 to 0% of the brightness of 23S-2018, respectively) was as follows: class I, 3%; class II, 21%; class III, 35%; class IV, 18%; class V, 16%; and class VI, 7%. A fine-resolution analysis of selected areas confirmed steep changes in accessibility on the 23S RNA to oligonucleotide probes. This is similar to the situation for the 16S rRNA. Indeed, no significant differences were found between the hybridization of oligonucleotide probes to 16S and 23S rRNA. Interestingly, indications were obtained of an effect of the type of fluorescent dye coupled to a probe on in situ accessibility. The results were translated into an accessibility map for the 23S rRNA of *E. coli*, which may be extrapolated to other bacteria. Thereby, it may contribute to a better exploitation of the high potential of the 23S rRNA for identification of bacteria in the future.

Probing with 16S rRNA-targeted oligonucleotides has become an important tool for the monitoring of microbial populations (3, 10). Fluorescence in situ hybridization (FISH) allows the identification of individual cells in complex environments (3). One of the main problems of FISH, besides low cellular ribosome content and impermeability of cell walls, is the inaccessibility of probe target sites due to the higher-order structure of the ribosome (6). Furthermore, despite its length of approximately 1,500 nucleotides, it is sometimes impossible to find suitable signature sites on the 16S rRNA for the identification of the organism(s) of interest. The 23S rRNA, with its length of approximately 3,000 nucleotides, would be the ideal alternative as a probe target molecule. Like the 16S rRNA, it is present in high copy number in all living cells. Its structure and function are highly conserved (13). A drawback is that there are currently only approximately 1,000 full-length 23S rRNA sequences in the databases, compared to more than 18,000 16S rRNA sequences (8). In the age of genome sequencing, it can safely be predicted that this gap will be closing. The availability of a sufficiently large database will allow researchers to exploit the high potential of the 23S rRNA for probe design, which is, considering only the average length of the 16S and the 23S rRNA, twice as large as that of the 16S rRNA. With a study on the in situ accessibility of the 23S rRNA of *Escherichia coli* to CY3-labeled oligonucleotides, we want to contribute to this development.

* Corresponding author. Mailing address: Celsiusstr. 1, D-28359 Bremen, Germany. Phone: 49 421 2028 934. Fax: 49 421 2028 790. E-mail: bfuchs@mpi-bremen.de.

MATERIALS AND METHODS

Cultivation and sequencing. *Escherichia coli* K-12 (DSM 30083^T; DSMZ—Deutsche Sammlung von Mikroorganismen und Zellkulturen GmbH, Braunschweig, Germany) was grown according to the DSMZ catalogue of strains. Cells were harvested in logarithmic growth phase at an optical density at 600 nm of 0.5 by centrifugation for 5 min at 4,500 × *g*. Cells were washed once with 1× phosphate-buffered saline (130 mM sodium chloride, 10 mM sodium phosphate buffer [pH 7.2]) and fixed with 4% paraformaldehyde as described previously (2). The 23S rRNA gene of *E. coli* was amplified directly from freshly harvested cells by PCR as described previously (12). The 5′ half of the 23S rDNA was amplified with primer pair 23-1V (5′-TTGTGAGGTTAAGCGACT-3′) and 23S-1534R (5′-TAGTGCCTCGTCATCACG-3′), and the 3′ half was amplified with pair 23S-1517V (5′-CGTGATGACGAGGCACTA-3′) and 23S-2904R (5′-CGGCG TTGTAAGGTTAAG-3′). After subsequent purification with the QIAquick PCR purification kit (Qiagen, Hilden, Germany), both strands of the PCR product were sequenced on a 377 DNA sequencer (Perkin-Elmer, Applied Biosystems, Foster City, Calif.) and on a Licor 4000 (MWG Biotech, Ebersberg, Germany). The sequence was deposited at the EMBL database under the accession number AJ278710.

Probe design. The standard probe set consisted of neighboring probes covering the full 23S rRNA of *E. coli*. For fine mapping, additional probes with overlapping target sites were designed. Self-complementarity of probes of more than three nucleotides was avoided. The standard probe length of 18 nucleotides was varied if the estimated dissociation temperature (T_d), according to the 4+2 formula of Suggs (11) [$T_d = 4 \cdot (G + C) + 2 \cdot (A + T)$], exceeded 60°C or was below 48°C (6). All probes used in this study are listed with their sequences and target positions in Table 1.

Probe labeling and quality control. Probes were synthesized monolabeled at the 5′ end with either CY3, carboxyfluorescein (FAM), or carboxytetramethylrhodamine (TAMRA) by Interactiva GmbH (Ulm, Germany). Aliquots of each probe were analyzed in a spectrophotometer (UV-1202; Shimadzu, Duisburg, Germany). The peak ratios of the absorption of DNA at 260 nm and the

TABLE 1. Sequences and relative fluorescence intensities of a set of oligonucleotide probes targeting the 23S ribosomal RNA of *E. coli* K-12

Probe name	*E. coli* position (5′→3′)[a]	Probe sequence (5′→3′)	Relative probe fluorescence (%)[b]	Brightness class
23S-1	1–18	ACGCTTAGTCGCTTAACC	34	IV
23S-19	19–36	CCAGGGCATCCACCGTGT	55	III
23S-37	37–54	CTTCATCGCCTCTGACTG	61	II
23S-55	55–72	ATCGCAGATTAGCACGTC	51	III
23S-73	73–90	ATCACCTCACCGACGCTT	52	III
23S-91	91–108	CCGGTTATAACGGTTCAT	27	IV
23S-109	109–126	TTCCCCATTCGGAAATCG	38	IV
23S-127	127–144	TGTCGAAACACACTGGGT	46	III
23S-145	145–163	GATTCAGTTAATGATAGTG	3	VI
23S-164	164–181	TCGCCTCATTAACCTATG	58	III
23S-182	182–199	TGTTTCAGTTCCCCCGGT	69	II
23S-200	200–217	TTCCTCGGGGTACTTAGA	33	IV
23S-218	218–235	AATCTCGGTTGATTTCTT	81	I
23S-236	236–252	CTCGCCGCTACTGGGGG	72	II
23S-253	253–269	GGGCTCCTCCCCGTTCG	57	III
23S-270	270–287	CACACTGATTCAGGCTCT	48	III
23S-288	288–305	GACGCTTCCACTAACACA	14	V
23S-306	306–323	GTATCGCGCGCCTTTCCA	61	II
23S-324	324–341	GTACGGGGCTGTCACCCT	63	II
23S-342	342–360	ACAATATGTGCATTTTTGT	13	V
23S-361	361–378	GCCCTACTCATCGAGCTC	68	II
23S-369	369–386	CGTGTCCCGCCCTACTCA	72	II
23S-387	387–404	TATTCAGACAGGATACCA	22	IV
23S-397	397–414	GGTCCCCCCATATTCAGA	74	II
23S-415	415–432	TATTTAGCCTTGGAGGAT	69	II
23S-433	433–450	CTATCGGTCAGTCAGGAG	67	II
23S-451	451–468	CCTCACGGTACTGGTTCA	66	II
23S-469	469–486	GGGTTCTTTTCGCCTTTC	77	II
23S-487	487–504	TTTTCACTCCCCTCGCCG	58	III
23S-505	505–522	TACACGGTTTCAGGTTCT	32	IV
23S-523	523–540	GCTCCCACTGCTTGTACG	79	II
23S-529	529–546	AAAGAGGCTCCCACTGCT	66	II
23S-547	547–564	GTACGCAGTCACCCCCAT	45	III
23S-560	560–577	CATTATACAAAAGGTACG	31	IV
23S-578	578–595	GAATATAAGTCGCTGACC	11	V
23S-596	596–613	TCGGTTAACCTTGCTACA	29	IV
23S-614	614–631	TCCCTTCGGCTCCCCTAT	66	II
23S-632	632–649	CCCAGTTAAGACTCGGTT	36	IV
23S-650	650–667	ATACCCTGCAACTTAACG	23	IV
23S-668	668–685	TCACCGGGTTTCGGGTCT	53	III
23S-686	686–703	AACCTGCCCATGGCTAGA	32	IV
23S-704	704–721	TAGTGTTACCCAACCTTC	23	IV
23S-722	722–739	TCGGTTCGGTCCTCCAGT	54	III
23S-731	731–748	CAACATTAGTCGGTTCGG	3	VI
23S-749	749–766	AGTCATCCGCTAATTTTT	14	V
23S-759	759–776	CCCAGCCACAAGTCATCC	48	III
23S-777	777–794	TTTGATTGGCCTTTCACC	58	III
23S-795	795–812	GAACCAGCTATCTCCCGG	61	II
23S-813	813–830	CTAAATAGCTTTCGGGGA	43	III
23S-831	831–848	GAATTCACGAGGCGCTAC	38	IV
23S-849	849–866	TGCTCTACCCCCGGAGAT	37	IV
23S-867	867–884	ACCCCCTTGCCGAAACAG	39	IV
23S-885	885–902	GGTTGGTAAGTCGGGATG	6	V
23S-903	903–920	TATTCGCAGTTTGCATCG	10	V
23S-921	921–938	CGTGATAACATTCTCCGG	3	VI
23S-930	930–947	TGTGTCTCCCGTGATAAC	37	IV
23S-939	939–955	ACCCGCCGTGTGTCTCC	49	III
23S-948	948–964	GACGTTAGCACCCGCCG	14	V
23S-956	956–973	TTCACGACGGACGTTAGC	4	VI
23S-965	965–982	GTTTCCCTCTTCACGACG	51	III
23S-974	974–991	GTCTGGGTTGTTTCCCTC	94	I
23S-992	992–1009	TTGGGACCTTAGCTGGCG	62	II
23S-1010	1010–1027	TCCCACTTAACCATGACT	56	III
23S-1028	1028–1045	GGGCCTTCCCACATCGTT	62	II
23S-1046	1046–1063	CCAACATCCTGGCTGTCT	53	III
23S-1064	1064–1081	ATGATGGCTGCTTCTAAG	42	III
23S-1082	1082–1100	GCTATTACGCTTTCTTTAA	42	III

Continued on next page

TABLE 1—*Continued*.

Probe name	*E. coli* position (5′→3′)[a]	Probe sequence (5′→3′)	Relative probe fluorescence (%)[b]	Brightness class
23S-1101	1118–1118	GGCCGACTCGACCAGTGA	65	II
23S-1137	1137–1154	CGGTGCATGGTTTAGCCC	59	III
23S-1155	1155–1172	GTGTCGCTGCCGCAGCTT	60	III
23S-1173	1173–1191	CCTACCCAACAACACATA	58	III
23S-1192	1192–1209	AGGCTTACAGAACGCTCC	49	III
23S-1210	1210–1227	CTCACAGGCCACCTTCAC	61	II
23S-1228	1228–1245	CTGATACCTCCAGCAACC	32	IV
23S-1246	1246–1263	ATGTCAGCATTCGCACTT	61	II
23S-1264	1264–1281	CCCGCTTTATCGTTACTT	66	II
23S-1282	1282–1299	CGGCGAGCGGGCTTTTCA	42	III
23S-1300	1300–1317	CAGGAACCCTTGGTCTTC	66	II
23S-1310	1310–1327	TAACGTTGGACAGGAACC	44	III
23S-1328	1328–1345	GACTCACCCTGCCCCGAT	68	II
23S-1336	1336–1353	TAGGGGTCGACTCACCCT	63	II
23S-1354	1354–1370	GCCTTTCGGCCTCGCCT	52	III
23S-1371	1371–1388	CTGTTTCCCATCGACTAC	59	III
23S-1389	1389–1407	CAAGTACAGGAATATTAAC	3	VI
23S-1408	1408–1425	CCCCCTTCGCAGTAACAC	64	II
23S-1426	1426–1443	AACATAGCCTTCTCCGTC	74	II
23S-1444	1444–1460	ACAACCGTCGCCCGGCC	31	IV
23S-1461	1461–1478	CTACACGCTTAAACCGGG	6	V
23S-1467	1467–1484	ACCAGCCTACACGCTTAA	7	V
23S-1479	1479–1496	TTTGCCTGGAAAACCAGC	1	VI
23S-1485	1485–1502	TCCGGATTTGCCTGGAAA	7	V
23S-1491	1491–1508	TGGTTTTCCGGATTTGCC	9	V
23S-1497	1497–1514	CAGCCTTGGTTTTCCGGA	83	I
23S-1509	1509–1526	GTCATCACGCCTCAGCCT	45	III
23S-1515	1515–1532	TGCCTCGTCATCACGCCT	56	III
23S-1524	1524–1541	GCACCGTAGTGCCTCGTC	6	V
23S-1533	1533–1551	TGTCGCTTCAGCACCGTAG	15	V
23S-1552	1552–1569	TCCTGGAAGCAGGGCATT	24	IV
23S-1570	1570–1587	CTGATGCTTAGAGGCTTT	10	V
23S-1588	1588–1605	GGTACGATTTGATGTTAC	6	V
23S-1606	1606–1623	CCACCTGTGTCGGTTTGG	64	II
23S-1615	1615–1632	TCTACCTGACCACCTGTG	58	III
23S-1633	1633–1650	TCAAGCGCCTTGGTATTC	65	II
23S-1642	1642–1659	CGAGTTCTCTCAAGCGCC	62	II
23S-1660	1660–1677	TTGCCTAGTTCCTTCACC	57	III
23S-1678	1678–1695	CGAAGTTACGGCACCATT	41	III
23S-1696	1696–1713	TATCAGCGTGCCTTCTCC	94	I
23S-1714	1714–1731	CAAGTCGCTTCACCTACA	26	IV
23S-1732	1732–1749	TGATTTCAGCTCCACGAG	17	V
23S-1750	1750–1767	CCAGCTGGTATCTTCGAC	59	III
23S-1768	1768–1786	TTTTAATAAACAGTTGCAG	36	IV
23S-1787	1787–1804	GTTTGCACAGTGCTGTGT	57	III
23S-1805	1805–1822	GTATACGTCCACTTTCGT	58	III
23S-1823	1823–1839	CGGGCAGGCGTCACACC	58	III
23S-1840	1840–1857	CAATTAACCTTCCGGCAC	53	III
23S-1858	1858–1875	CGCTACCGCTAACCCCAT	12	V
23S-1876	1876–1893	GGCTTCGATCAAGAGCTT	8	V
23S-1894	1894–1910	CGGCCGCCGTTTACCGG	35	IV
23S-1911	1911–1928	TTAGGACCGTTATAGTTA	8	V
23S-1929	1929–1946	ACAAGGAATTTCGCTACC	56	III
23S-1936	1936–1953	TTACCCGACAAGGAATTT	28	IV
23S-1954	1954–1971	ATTCGTGCAGGTCGGAAC	59	III
23S-1965	1965–1982	ATCATTACGCCATTCGTG	58	III
23S-1983	1983–1999	GTGGAGACAGCCTGGCC	34	IV
23S-2000	2000–2017	AATTTCACTGAGTCTCGG	41	III
23S-2018	2018–2035	CATCTTCACAGCGAGTTC	100	I
23S-2036	2036–2053	CTTGCCGCGGGTACACTG	45	III
23S-2054	2054–2071	TTCACGGGGTCTTTCCGT	50	III
23S-2072	2072–2089	GTCAAGCTATAGTAAAGG	3	VI
23S-2090	2090–2107	CAAGGCTCAATGTTCAGT	3	VI
23S-2099	2099–2116	CCTACACATCAAGGCTCA	41	III
23S-2108	2108–2125	CCCACCTATCCTACACAT	63	II
23S-2117	2117–2134	TCAAAGCCTCCCACCTAT	22	IV
23S-2126	2126–2143	GTCCACACTTCAAAGCCT	3	VI

Continued on next page

TABLE 1—*Continued*.

Probe name	*E. coli* position (5′→3′)[a]	Probe sequence (5′→3′)	Relative probe fluorescence (%)[b]	Brightness class
23S-2144	2144–2161	GGCTCCATGCAGACTGGC	3	VI
23S-2162	2162–2179	GGGTGGTATTTCAAGGTC	7	V
23S-2180	2180–2199	TTAGAACATCAAACATTAAA	1	VI
23S-2200	2200–2217	CCGGATTACGGGCCAACG	9	V
23S-2218	2218–2235	CCAGACACTGTCCGCAAC	48	III
23S-2227	2227–2244	AACTACCCACCAGACACT	48	III
23S-2236	2236–2253	CCCCAGTCAAACTACCCA	81	I
23S-2245	2245–2262	AGGAGACCGCCCCAGTCA	59	III
23S-2254	2254–2271	CTCTTTAGGAGGAGACCG	10	V
23S-2263	2263–2280	CCTCCGTTACTCTTTAGG	47	III
23S-2272	2272–2289	CTTCGTGCTCCTCCGTTA	75	II
23S-2290	2290–2307	CGACCAGGATTAGCCAAC	24	IV
23S-2308	2308–2325	CACTAACCTCCTGATGTC	61	II
23S-2326	2326–2343	AGCTGGCTTATGCCATTG	50	III
23S-2344	2344–2361	CCGTCACGCTCGCAGTCA	71	II
23S-2362	2362–2379	CTTTCGCACCTGCTCGCG	64	II
23S-2380	2380–2397	CCGGATCACTATGACCTG	62	II
23S-2398	2398–2415	CCCTTCCATTCAGAACCA	63	II
23S-2416	2416–2433	TTATCCGTTGAGCGATGG	31	IV
23S-2434	2434–2451	TTATCCCCGGAGTACCTT	45	III
23S-2452	2452–2469	TTGGGCGGTATCAGCCTG	23	IV
23S-2470	2470–2487	CGCCGTCGATATGAACTC	10	V
23S-2488	2488–2505	CATCGAGGTGCCAAACAC	13	V
23S-2506	2506–2523	CAGGATGTGATGAGCCGA	16	V
23S-2514	2514–2531	TTCAGCCCCAGGATGTGA	14	V
23S-2532	2532–2549	CATACCCTTGGGACCTAC	19	V
23S-2542	2542–2559	GGCGAACAGCCATACCCT	19	V
23S-2560	2560–2577	TCGCGTACCACTTTAAAT	43	III
23S-2578	2578–2595	CGACGTTCTAAACCCAGC	45	III
23S-2596	2596–2613	AGGGACCGAACTGTCTCA	55	III
23S-2614	2614–2630	CAGCGCCCACGGCAGAT	23	IV
23S-2631	2631–2648	CAGCCCCCCTCAGTTCTC	67	II
23S-2649	2649–2666	GTCCTCTCGTACTAGGAG	51	III
23S-2667	2667–2684	AGTGATGCGTCCACTCCG	44	III
23S-2685	2685–2702	CATGACAACCCGAACACC	9	V
23S-2703	2703–2720	ACCGGGCAGTGCCATTGG	21	IV
23S-2721	2721–2738	TCTCTTCCGCATTTAGCT	59	III
23S-2739	2739–2756	AGATGCTTTCAGCACTTA	5	VI
23S-2757	2757–2774	GGGGCAAGTTTCGTGCTT	27	IV
23S-2775	2775–2792	TCAGGGAGAACTCATCTC	37	IV
23S-2781	2781–2798	TAAGTCTCAGGGAGAACT	12	V
23S-2799	2799–2816	CGTTCCTTCAGGAGACTC	51	III
23S-2811	2811–2828	CGTCGTCTTCAACGTTCC	60	III
23S-2829	2829–2846	CACCCGGCCTATCAACGT	60	III
23S-2840	2840–2857	CTGCGCTTACACACCCGG	58	III
23S-2858	2858–2875	GGTTAGCTCAACGCATCG	60	III
23S-2865	2865–2882	TAGTACCGGTTAGCTCAA	48	III
23S-2883	2883–2900	TTAAGCCTCACGGTTCAT	44	III
23S-2887	2887–2904	AAGGTTAAGCCTCACGGT	36	IV

[a] *E. coli* position according to the numbering of Brosius et al. (5).
[b] Fluorescence intensities expressed as a percentage of that of the brightest probe detected, 23S-2018.

absorption of the respective dye were determined in order to check the labeling quality of the oligonucleotides (6).

FISH. As described previously (6), approximately 4×10^6 cells were hybridized in 80 μl of buffer containing 0.9 M sodium chloride, 0.01% sodium dodecyl sulfate, 20 mM Tris-HCl (pH 7.2), and 1.5 ng of fluorescent probe μl^{-1} at 46°C for 2 h. Subsequently, cells were pelleted by centrifugation for 2 min at 4,000 × *g*, the supernatant was discharged, and the cells were resuspended in 100 μl of hybridization buffer containing no probe. After being washed for 20 min at 46°C, samples were mixed with 300 μl of 1× phosphate-buffered saline (pH 9.0 for FAM-labeled probes), immediately placed on ice, and analyzed within 3 h.

Flow cytometry. Probe-conferred fluorescence of hybridized cells was quantified by a FACStar Plus flow cytometer (Becton Dickinson, Mountain View, Calif.). For CY3- and TAMRA-labeled probes, the argon ion laser was tuned to an output power of 750 mW at 514 nm. Forward-angle light scatter (FSC) was detected with a BP 530/30 (Becton Dickinson) band pass filter. Fluorescence (FL1) was detected with a 620 (±60)-nm band-pass filter (Gesellschaft für dünne Schichten mbH; Hugo Anders, Nabburg, Germany). FAM-labeled probes were excited with the 488-nm line of the argon ion laser at an output power of 500 mW. FSC was then detected through a BP 488/10 (Becton Dickinson) band-pass filter, and FL1 was detected through a BP 530/30 band-pass filter.

The system threshold was usually set on FSC. FAM-labeled probes were measured with 1× PBS (pH 9.0), and CY3- and TAMRA-labeled probes were measured with deionized water as sheath fluid. Polychromatic, 0.5-μm polystyrene beads (Polysciences, Warrington, Pa.) were used to check the stability of the optical alignment of the flow cytometer and to standardize the fluorescence intensities of cells hybridized with CY3-labeled probes. For quantification of cells hybridized with FAM-labeled probes, 0.5-μm yellow-green polystyrene beads were used.

Data acquisition and processing. The parameters FSC and FL1 were recorded as pulse height signals (4 decades in logarithmic scale each), and for each measurement 10,000 events were stored in list mode files. Subsequent analysis was done with the CellQuest software (Becton Dickinson). Probe-conferred fluorescence was determined as the median of the FL1 values of single cells recorded in a gate that was defined in an FSC-versus-FL1 dot plot. Fluorescence of cells was corrected by subtraction of background fluorescence of negative controls and standardized to the fluorescence of reference beads. All values were finally expressed relative to the value for the brightest probe detected.

Probe-conferred fluorescence intensities were recorded for triplicate samples. Each replicate represents independent cell hybridization. Only triplicates with a coefficient of variation of less than 10% were accepted; otherwise, the quantification was repeated. The mean of triplicate measurements is given in Table 1.

Comparison of 16S rRNA and 23S rRNA. A total of 13 probes were chosen to compare 16S rRNA and 23S rRNA accessibilities, with six probes targeting the 16S rRNA and seven targeting the 23S rRNA. The former were taken from the study of Fuchs and colleagues (6). Since the 16S rRNA was previously screened with FAM-labeled oligonucleotides and the 23S rRNA in this study was screened with CY3-labeled probes, probe batches labeled with FAM and CY3 and additionally with a third dye, TAMRA, were quantified. All probes were hybridized against the same *E. coli* batch, and all fluorescence intensities were standardized to the fluorescence of the brightest probe on the 16S rRNA, Eco1482.

RESULTS AND DISCUSSION

23S rRNA accessibility. The brightest signal after hybridization to the 23S rRNA on *E. coli* was recorded for probe 23S-2018 binding to positions 2018 to 2035 (5). Consequently, fluorescence intensities from all probes were expressed as a percentage of that of 23S-2018 and grouped into six brightness classes (Table 1). Class I probes showed 100 to 81% of the 23S-2018 probe's fluorescence, class II showed 80 to 61%, class III showed 60 to 41%, class IV showed 40 to 21%, class V showed 20 to 6%, and class VI showed 5 to 0% (6). An additional five probes yielded signal intensities of class I: 23S-218 (81%), 23S-974 (94%), 23S-1497 (83%), 23S-1696 (94%), and 23S-2236 (81%) (Fig. 1). More than half of the probes tested fell in classes II and III. They targeted coherent areas, e.g., between helices 2 and 7, 13 and 16, 19 and 24, 31a and 32, 41 and 46, 47 and 52, 54 and 56, 59 and 62, 66 and 67, 72 and 74, 84 and 88, 92 and 93, 94 and 95, and 99 and 101 (Fig. 1). About a third of the probes quantified had medium (class IV) (33 probes) to low (class V) (30 probes) accessibility on the 23S ribosomal RNA. Most clustered, e.g., around helix 31, the long helix 38, between helices 54 and 59, at helices 63, 68, and 69, in the area encompassing helices 89 to 92, and at helix 96. The rest were spread over the 23S rRNA molecule (Fig. 1). Twelve probes yielded signals hardly above background levels (relative fluorescence, 0 to 5%). These highly inaccessible sites are at helices 10, 35, 38, 38, 53, 58, 75, 76, 78, and 97 (Fig. 1). Hybridization of these class VI probes at 37 and 41°C did not enhance the probe-conferred signals (data not shown).

Fine mapping. Four regions showing steep changes in accessibility were examined at a higher spatial resolution with additional probes (Fig. 1; Table 1). The class III probe 23S-939, with a relative fluorescence of 49%, is surrounded by the class VI probes 23S-921 (relative fluorescence, 3%) and 23S-956 (4%). The latter is directly adjacent to one of the brightest probes, 23S-974 (94%). Three additional probes that targeted intermediate sites showed fluorescence intensities between the extreme values: for 23S-930, 37%; for 23S-948, 14%; and for probe 23S-965, 51% relative fluorescence.

A similar situation is found between positions 2090 and 2143. There, the class II probe 23S-2108 (relative fluorescence, 63%) is flanked by two sites with low accessibility (23-2090 and 23S-2126, both at 3%). The fine mapping with probes 23S-2099 and 23S-2117 revealed intermediate accessibilities of 41 and 22%, respectively. In the third region examined, the bright probes 23S-2236 (81%) and 23S-2272 (75%) frame the dim probe 23S-2254 (10%). All three probes used for fine resolution of this area, 23S-2227 (48%), 23S-2245 (60%), and 23S-2263 (47%), are class III. Finally, a very steep increase in accessibility could be detected at helix 58a. The 5′ end of helix 58 and 58a is targeted by four probes (23S-1467, 23S-1479, 23S-1485, and 23S-1491) with a maximal relative fluorescence of 9% (23S-1491). The adjacent probe 23S-1497 showed high accessibility (83%). When the target site was moved further towards the 3′ end of the 23S rRNA, the signals dropped again to a class III (23S-1509, 45%, and 23S-1515, 56%) and finally to a class V (23S-1524, 6%, and 23S-1533, 15%) level at the 3′ end of helix 58.

Current structure models of the large subunit of the ribosome, such as the probably most elaborate model, the 2.4-Å-resolution crystal structure for *Haloarcula marismortui* (4) or the 7.5-Å cryo-electron microscopic reconstruction for *E. coli* (9), provide some possible explanations for sites with low accessibility. The helices 38, 39, and 89, all of which show class V accessibility, are apparently at least partly involved in tight bonds to the 5S ribosomal RNA (see reference 9 and references therein). Interactions with ribosomal proteins may be responsible for the low signals as well, e.g., the interaction of protein L1 with the distal part of helix 68, probes 23S-2117 and 23S-2162 (9). The ribosomal protein L6 presumably causes low levels of fluorescence at the distal part of helix 89. Other parts of the 23S rRNA, such as the helices 75 and 76, are located deeper within the 50S subunit. The respective probes may be hindered in penetrating to the target site. However, the accessibility data presented in our study were obtained on fixed *E. coli* cells, and therefore attempts to correlate probe accessibility with structural data should be done with great care.

Comparison of 16S and 23S rRNA accessibility. At first glance, the 23S rRNA is more accessible to oligonucleotide probes than the 16S rRNA in the small subunit of the ribosome. Almost 60% of all probes quantified could be grouped in the brightness classes I to III, compared to only 39% on the 16S rRNA. Vice versa, only 23% of the 23S rRNA probes belonged to class V or VI, whereas 32% of probes targeting the 16S rRNA show relatively low binding. However, it must be considered that the study on the in situ accessibility of the 16S rRNA of *E. coli* was performed with a FAM-labeled oligonucleotide probe, whereas the present study used CY3-labeled probes. CY3 is currently the most-used label in FISH, since it has a high absorption coefficient and a high quantum yield, shows little bleaching and, in contrast to FAM, is pH insensitive. Even though CY3 is a stronger fluorophor than FAM, relative fluorescence values should not be influenced by the change of label.

To nevertheless investigate a potential influence of the fluorescent marker on relative probe binding, a comparison of FAM, CY3, and additionally TAMRA was done with a set of oligonucleotides encompassing 16S and 23S rRNA-targeted probes of different brightness classes. Quantification of the FAM-labeled probes (Fig. 2) showed that Eco1482 was the brightest probe among all probes measured. The FAM-labeled

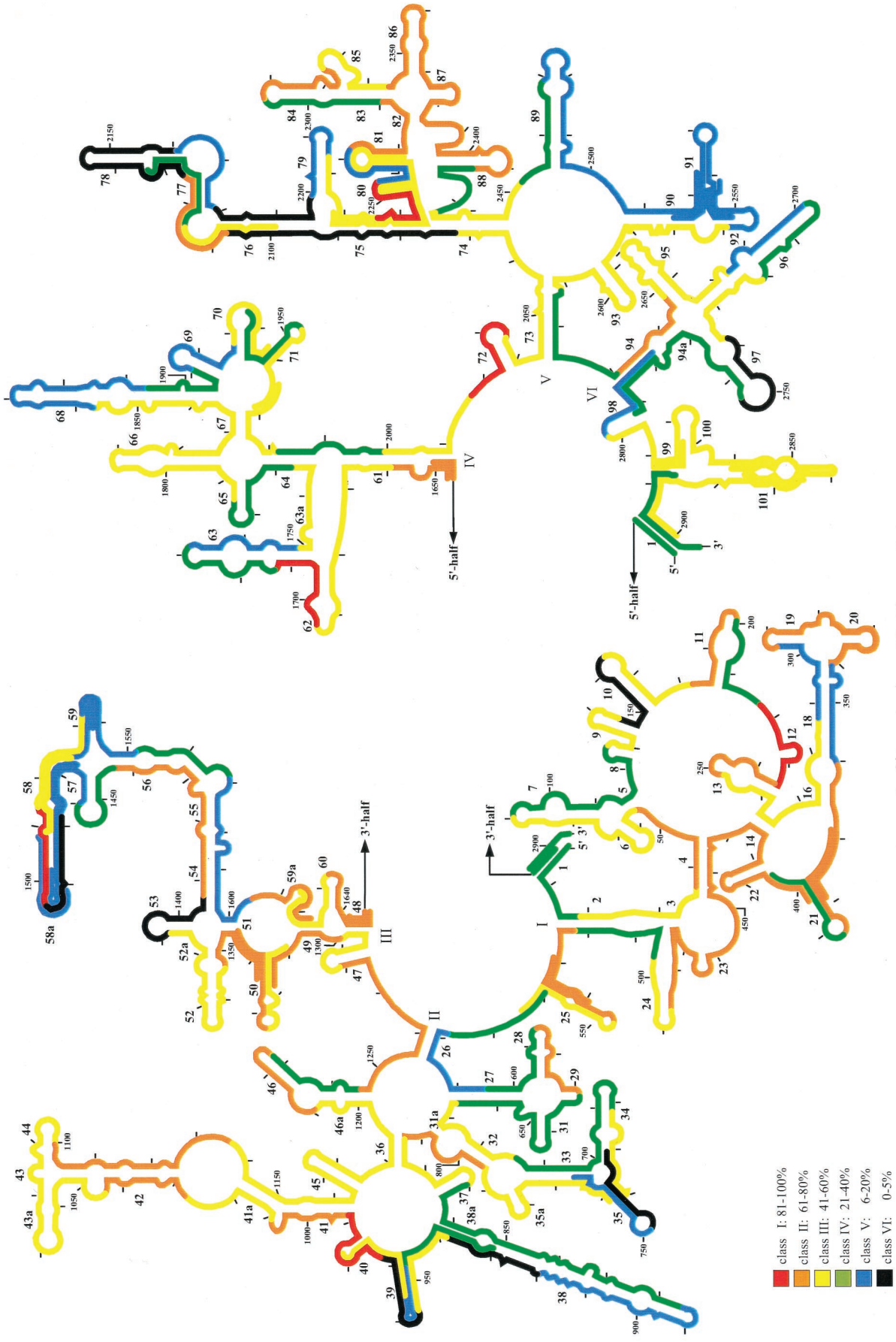

FIG. 1. Fluorescence intensities of all oligonucleotide probes, standardized to that of the brightest probe, 23S-2018, shown in a 23S rRNA secondary structure model (7). The 5′ and the 3′ halves of the 23S rRNA are depicted on the left and right, respectively. The color coding indicates differences in the level of probe-conferred fluorescence. Additional probes for a detailed analysis of four regions with steep changes in accessibility are included in the graphs.

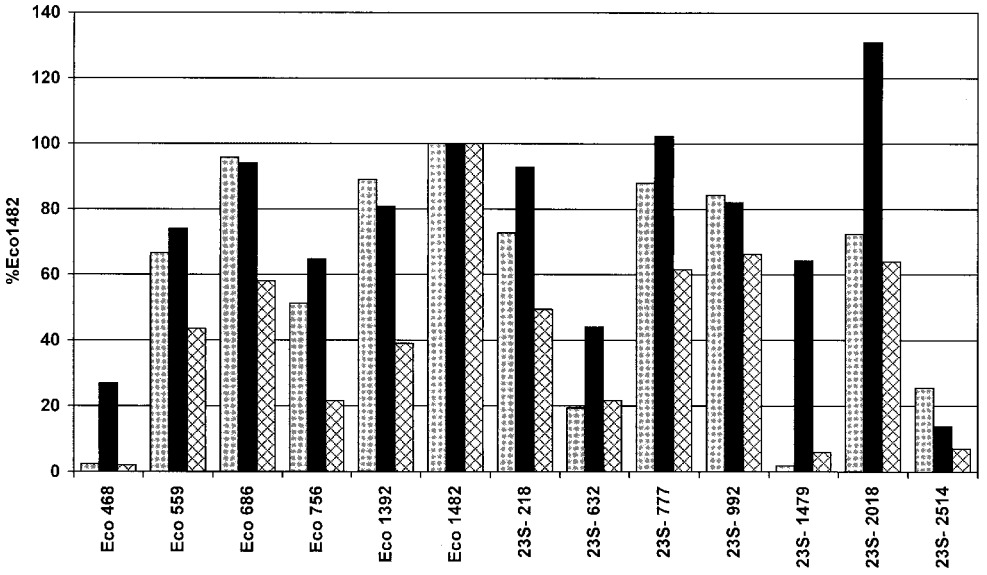

FIG. 2. Comparison of 16S and 23S rRNA-targeted oligonucleotide probes, labeled with FAM (gray bars), CY3 (black bars), and TAMRA (cross-hatched bars). All fluorescence intensities are calibrated to that of the respectively labeled probe Eco1482.

16S rRNA-targeted probes Eco686 (96%) and Eco1392 (89%) were still brighter than the brightest FAM-labeled probe targeting 23S rRNA, 23S-777 (88%). The lowest fluorescence intensities, with 2% relative fluorescence each, were found for probes Eco468 on the 16S rRNA and 23S-1479 on the 23S rRNA. For TAMRA-labeled probes the picture was similar. The brightest signals could be obtained from Eco1482, followed by 23S-992 (66%), 23S-2018 (64%), and 23S-777 (62%). Probes Eco468 (2%) and 23S-1479 (6%) once again were associated with low accessibility. The CY3-labeled probes, however, generally showed higher relative fluorescence than the FAM- and TAMRA-labeled oligonucleotides. With CY3 as the label, the brightest 23S rRNA-targeted probe, 23S-2018 (131%), showed a higher fluorescence intensity than Eco1482, the brightest probe with FAM and TAMRA, on which all fluorescence values were normalized. Furthermore, probes Eco486, 23S-1479, and 23S-632 showed considerably better relative binding when labeled with CY3 than with FAM and TAMRA (Fig. 2). Apparently there is a link between the type of label and accessibility. The explanation for this phenomenon may be the more linear chemical structure of the carbocyanine dye CY3 compared to those of the two-dimensional triphenylmethane dyes FAM and TAMRA. A one-dimensional dye molecule might penetrate better into the tight higher-order structure of the ribosome (4). Fluorophor-dependent quenching at the various target sites and differences in the charging or charge distributions of the different dye molecules may be alternative explanations. We have recently started a study on the in situ accessibility of the 16S rRNA of *E. coli* for CY3-labeled oligonucleotide probes to further investigate this phenomenon in comparison to the earlier data of Fuchs and colleagues (6).

We also investigated whether the accessibility of 23S rRNA target sites is linked to their mean phylogenetic conservation. The coefficient r^2 was found to be 3.7%. Obviously, as previously shown for the 16S rRNA, there is no significant correlation between these two properties (6) (Fig. 3).

Conclusions. The 23S rRNA has twice as many potential probe target sites as the 16S rRNA, for which it is sometimes difficult to find diagnostic sequences unique to a chosen group of organisms. It has been pointed out (1) that even in cases where a 16S rRNA-targeted probe can still be designed, a 23S

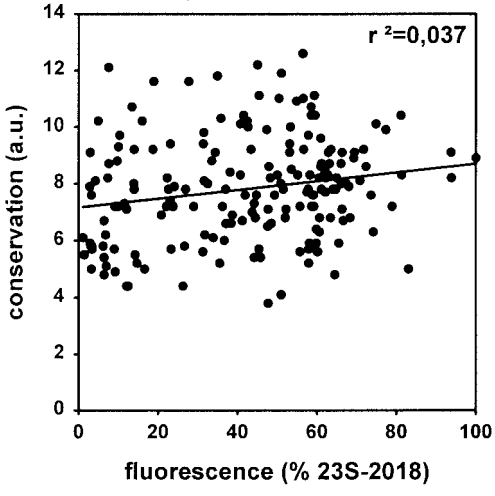

FIG. 3. Correlation of the conservation value and relative fluorescence intensity of each probe measured in the study. Conservation values were calculated by averaging the conservation values of single nucleotide positions comprising the probe target position. The conservation values are based on the fraction of available bacterial sequences that share an identical nucleotide in a particular alignment position (ARB software; Department of Microbiology, Technische Universität München, Munich, Germany [http://www.mikro.biologie.tu-muenchen.de]). They are expressed in arbitrary units (a.u.), in which low values indicate low evolutionary conservation.

rRNA-targeted probe of similar or identical specificity is valuable in increasing the significance of in situ identification. Due to the high evolutionary conservation of this molecule, the 23S rRNA in situ accessibility map for *E. coli* can, within certain limits, as previously discussed for the 16S rRNA (6), be extrapolated to other microorganisms. We hope that this study supports a more intensive use of the 23S rRNA as a target for FISH in the future.

ACKNOWLEDGMENTS

This study was supported by grants of the Deutsche Forschungsgemeinschaft Am 73/3-1 and the Max Planck Society.

We thank Nenad Ban and Pavel Baranov for helpful discussions on the structure of the 23S rRNA and Jörg Wulf and Daniela Lange for technical assistance.

REFERENCES

1. **Amann, R., and W. Ludwig.** 1994. Typing in situ with probes, p. 115–135. *In* F. G. Priest, A. Ramos-Cormenzana, and B. J. Tindall (ed.), Bacterial diversity and systematics. Plenum, New York, N.Y.
2. **Amann, R. I., L. Krumholz, and D. A. Stahl.** 1990. Fluorescent-oligonucleotide probing of whole cells for determinative, phylogenetic, and environmental studies in microbiology. J. Bacteriol. **172:**762–770.
3. **Amann, R. I., W. Ludwig, and K. H. Schleifer.** 1995. Phylogenetic identification and in situ detection of individual microbial cells without cultivation. Microbiol. Rev. **59:**143–169.
4. **Ban, N., P. Nissen, J. Hansen, P. B. Moore, and T. A. Steitz.** 2000. The complete atomic structure of the large ribosomal subunit at 2.4 angstrom resolution. Science **289:**905–920.
5. **Brosius, J., T. J. Dull, D. D. Sleeter, and H. F. Noller.** 1981. Gene organization and primary structure of a ribosomal RNA operon from *Escherichia coli*. J. Mol. Biol. **148:**107–127.
6. **Fuchs, B. M., G. Wallner, W. Beisker, I. Schwippl, W. Ludwig, and R. Amann.** 1998. Flow cytometric analysis of the in situ accessibility of *Escherichia coli* 16S rRNA for fluorescently labeled oligonucleotide probes. Appl. Environ. Microbiol. **64:**4973–4982.
7. **Gutell, R. R., N. Larsen, and C. R. Woese.** 1994. Lessons from an evolving rRNA: 16S and 23S structures from a comparative perspective. Microbiol. Rev. **58:**10–26.
8. **Maidak, B. L., J. R. Cole, T. G. Lilburn, C. T. J. Parker, P. R. Saxmann, J. M. Stredwick, G. M. Garrity, G. J. Olsen, S. Pramanik, T. M. Schmidt, and J. M. Tiedje.** 2000. The RDP (Ribosomal Database Project) continues. Nucleic Acids Res. **28:**173–174.
9. **Mueller, F., I. Sommer, P. Baranov, R. Matadeen, M. Stoldt, J. Wohnert, M. Gorlach, M. van Heel, and R. Brimacombe.** 2000. The 3D arrangement of the 23 S and 5 S rRNA in the *Escherichia coli* 50 S ribosomal subunit based on a cryo-electron microscopic reconstruction at 7.5 angstrom resolution. J. Mol. Biol. **298:**35–59.
10. **Olsen, G. J., D. J. Lane, S. J. Giovannoni, N. R. Pace, and D. A. Stahl.** 1986. Microbial ecology and evolution: a ribosomal rRNA approach. Annu. Rev. Microbiol. **40:**337–365.
11. **Suggs, S. V., T. Hirose, T. Miyake, E. H. Kawashima, M. J. Johnson, K. Itakura, and R. B. Wallace.** 1981. Use of synthetic oligodeoxyribonucleotides for the isolation of specific cloned DNA sequences, p. 683–693. *In* D. Brown and C. F. Fox (ed.), Developmental biology using purified genes. Academic Press, Inc., New York, N.Y.
12. **Wallner, G., B. Fuchs, S. Spring, W. Beisker, and R. Amann.** 1997. Flow sorting of microorganisms for molecular analysis. Appl. Environ. Microbiol. **63:**4223–4231.
13. **Woese, C. R.** 1987. Bacterial evolution. Microbiol. Rev. **51:**221–271.